Fusion Engineering and Design 89 (2014) 2868–2874

Contents lists available at ScienceDirect

Fusion Engineering and Design

journal homepage: www.elsevier.com/locate/fusengdes

Computational studies of thermoelectric MHD driven liquid lithium flow in metal trenches

Wenyu Xu*, Davide Curreli, David N. Ruzic

Department of Nuclear, Plasma, and Radiological Engineering, University of Illinois at Urbana Champaign, Urbana, IL 61801, United States

HIGHLIGHTS

- We modeled the thermoelectric driven liquid lithium flow in open surface duct with the existence of external magnetic field and surface heating.
- The average flow velocity peaks at a critical magnetic field and then decreases with an inverse law in the range of tokamak-relevant fields.
- The flow velocity increases with a square-root law versus an increasing heat flux.
- Heat transfer coefficients higher than >4000 W/m^2 K are needed for the device in order to withstand heat fluxes of 10 MW/m^2.

ARTICLE INFO

Article history:
Received 11 December 2013
Received in revised form 10 June 2014
Accepted 12 June 2014
Available online 30 June 2014

Keywords:
Liquid lithium
MHD
Thermoelectric
Heat transfer
Limiter and divertor
Plasma facing component

ABSTRACT

The LiMIT system (Lithium/Metal Infused Trenches) is an innovative plasma-facing component for tokamak divertors, recently proposed at the University of Illinois. Thanks to the coupling of two metals having different Seebeck coefficients, the device is able to generate internal thermoelectric currents as a response to an incoming heat flux from the plasma. One of the two metals is liquid lithium and the second metal is a solid composing the trenches (tungsten, or molybdenum, or stainless steel, etc.). Together with the high toroidal magnetic field, the liquid lithium is propelled by a JxB electrodynamic force inside the solid trenches. In the present work we present a numerical characterization of the device. The diffusion–advection of heat is solved together with the Navier–Stokes equations forced by the JxB electrodynamic force, comprising the thermoelectric contribution. We report parametric plots to show the influence of the toroidal magnetic field and of the plasma heat flux. It is found that the average flow velocity of the liquid lithium peaks at a critical magnetic field, always lower than 1.0 T, and then decreases with an inverse law in the range of tokamak-relevant fields. The flow velocity of the lithium increases with a square-root law versus an increasing heat flux. The heat transfer coefficient of the cooling channels is parametrically investigated, revealing that coefficients higher than >4000 W/m^2 K are needed for the device in order to withstand heat fluxes of 10 MW/m^2.

1. Introduction

As we come closer to realizing fusion as a viable power source, many machines which have made significant progress in plasma heating and power find that removing heat from the divertor region has become a challenging problem. Peak heat fluxes up to 10 MW/m^2 are typical these days for machines, and if there is an ELM event or a disruption, then the flux can be even higher. Solid plasma facing components (PFC) materials such as carbon and tungsten suffer from permanent damage due to huge thermal stresses. Flowing liquid metals have been proposed as possible alternatives, since they offer a number of attractive advantages with respect to solid first walls. Traditional solid materials suffer of a number of problems like sputtering, fuzz growth, helium retention, bubble formation, dust, debris release, etc. Especially for high-Z materials like tungsten, the contamination caused to the plasma is critical, being source of high radiative bremsstrahlung losses. Several options have been considered, such as liquid lithium, or Sn–Li eutectics [1,2]. Among all the possible candidates, lithium has drawn a lot of interest recently, acting as a beneficial and active surface with regard to the plasma. Significant improvements of the plasma performance have been reported, both on tokamaks (TFTR [3], FTU [4], NSTX, etc.), stellarators (TJ-II), and reversed field pinches (RFX). Lithium offers the possibility to have a low recycling

* Corresponding author. Tel.: +1 2174194338.
E-mail address: xuwenyu1986@gmail.com (W. Xu).

http://dx.doi.org/10.1016/j.fusengdes.2014.06.008
0920-3796/

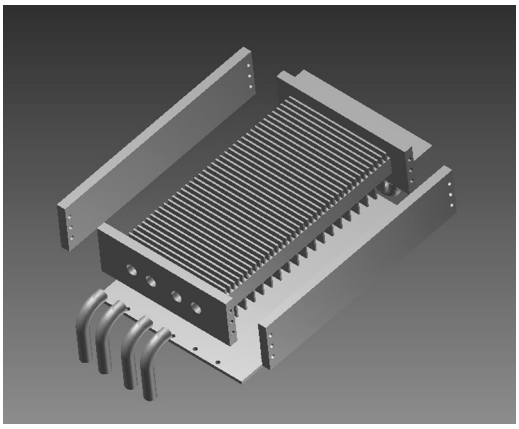

Fig. 1. CAD drawing of LiMIT.

wall [5,6], with improvements such as higher confinement time, higher plasma temperature and density, ELMs suppression (for tokamaks), and lower Z-effective.

At the University of Illinois at Urbana-Champaign (UIUC), a liquid-metal plasma-facing component called LiMIT (Lithium-Metal Infused Trenches) [7] has been developed and tested [8]. LiMIT has also been tested in the Chinese HT-7 superconducting tokamak [9]. LiMIT uses thermoelectric magnetohydrodynamics forces [10] to drive liquid lithium inside many narrow parallel trenches made of stainless steel (or molybdenum) with millimeter thick gaps between them. The feasibility of the TEMHD drive was proved for the first time at the University of Illinois [11] after inception tests on lithium walls done on the CDX-U spherical tokamak [12] and the temperature change of liquid lithium due to TEMHD driven swirling flow has been discussed [13]. A CAD drawing of LiMIT is reported in Fig. 1. The trenches of LiMIT are oriented along the poloidal direction of the torus, so that they are transversally crossed by the toroidal magnetic field. Once a temperature gradient is established between the top and bottom of the trench from the plasma hitting the lithium surface, a thermoelectric current is generated in the direction of the temperature gradient. The thermoelectric current drives the liquid inside the trench thanks to the JxB force originated from the interaction of the thermoelectric current with the toroidal field. The flow is self-driven by the instantaneous thermal gradient, hence resulting self-adaptive against the heat flow received from the plasma.

In the present paper we present a numerical characterization of LiMIT, done using COMSOL. The periodicity of the device suggests focusing the analysis on a single trench. In Section 2 we present the physical model. The diffusion–advection of heat is solved together with the Navier–Stokes equations forced by the volumetric JxB electrodynamic force; the current density is obtained from a generalized Ohm Law comprising the thermoelectric contribution. We verify the numerical solution against the semi-analytical case of a Hartmann flow in an infinite rectangular channel with an open surface. In Section 3 we present the results of the characterization. For each case, we solve the full 3D problem and calculate the flow velocity, the temperature, the electric potential, the current density, and the specific force. We report the average flow velocity and the maximum temperature on top of the trenches, versus the toroidal magnetic field and the plasma heat flux. We compare the results with a previous 1D analytic model [7], finding qualitative agreement. The influence of the heat transfer coefficient of the cooling channels and the influence of the trench height are parametrically investigated, revealing that coefficients higher than >5000 W/m^2 K are needed to withstand heat fluxes of 10 MW/m^2. Smaller trenches are better to increase the flow velocity of liquid lithium. Finally, we report a transient simulation of LiMIT in a 10 s plasma discharge in HT-7 like limiter configuration.

2. Model description

The commercial code COMSOL has been used to solve the thermoelectric-driven flow of liquid lithium in open metal trenches. The continuity and momentum of the liquid metal is described by the incompressible body-forced Navier–Stokes equations:

$$\nabla \times \mathbf{u} = 0. \tag{1}$$

$$\rho \frac{\partial \mathbf{u}}{\partial t} + \rho \mathbf{u} \times \nabla \mathbf{u} = -\nabla p + \mu \nabla^2 \mathbf{u} + \mathbf{j} \times \mathbf{B} \tag{2}$$

where $\mathbf{u}$ is the flow velocity, p is the pressure, ρ is lithium density, μ is the dynamic viscosity, and the $\mathbf{j}$x$\mathbf{B}$ term is the electrodynamic force acting on the liquid metal in presence of the magnetic field $\mathbf{B}$. The current density is obtained from the generalized quasi-static Ohm Law:

$$\nabla \times \mathbf{j} = 0. \tag{3}$$

$$\mathbf{j} = \sigma(-\nabla\phi + \mathbf{u} \times \mathbf{B} - S\nabla T) \tag{4}$$

where σ is the electrical conductivity, ϕ the electric potential, S the Seebeck coefficient (or "thermopower") of the material, and T the temperature. The temperature is found from the power balance:

$$\rho C_p \frac{\partial T}{\partial t} + \rho C_p \mathbf{u} \times \nabla T = \nabla \times \mathbf{q} + P_J \approx \nabla \times \mathbf{q} \tag{5}$$

$$\mathbf{q} = -k\nabla T + ST\mathbf{j} \approx -k\nabla T \tag{6}$$

where C_p is the heat capacity, and $\mathbf{q}$ the local thermal flux, k the thermal conductivity. In Eqs. (5) and (6) the Joule heating P_J and the Peltier heat flux $ST\mathbf{j}$ are second order effects, and can be neglected.

The solver has been verified on a simple case, the thermoelectric MHD flow on an infinite rectangular trench with an open surface. Analytical results have been obtained by Shercliff [10] for the 1D case. Fig. 2 shows our calculated results, obtained for a liquid lithium trench of 10 × 1.0 × 20 mm facing a solid stainless steel wall of the same size. The top surface uses a slip wall boundary condition, and constant temperature at 573 K. The bottom surface is a no-slip boundary at uniform temperature of 473 K. The external sides of the liquid part and of the solid part use symmetric boundary conditions. The inlet and the outlet use the periodic boundary conditions, to mimic the infinite-long trench. A transverse magnetic field of 1.0 T is set parallel to x. The results are compared to Shercliff's model. As expected, the velocity at the center of the channel is the same as predicted by Shercliff (see the overlapping black and red lines in the top right figure). However, the value close to the boundaries departs from Shercliff's solution. The velocity along the y direction has a peak value close to the bottom wall and decreases close to the top surface. This is reasonable, and is due by the three-dimensionality of the current density profile. In fact, near the top surface the current density vector becomes parallel to the top surface and to the magnetic field, so the Lorentz force becomes weaker there.

The model does not take into account the following phenomena, which may be relevant depending upon the conditions. Effects related to non-uniform magnetic fields are neglected, like curvature of the magnetic lines and $1/R$ dependence typical of tokamaks. The magnetic field is assumed to be constant in the small volume of the device. The density, thermal conductivity, electric conductivity, viscosity are assumed to be constants. The position of the grounded electrode is chosen to be at the edge. The effect of impurities (like LiD and LiT) in liquid lithium has not been considered, due to the

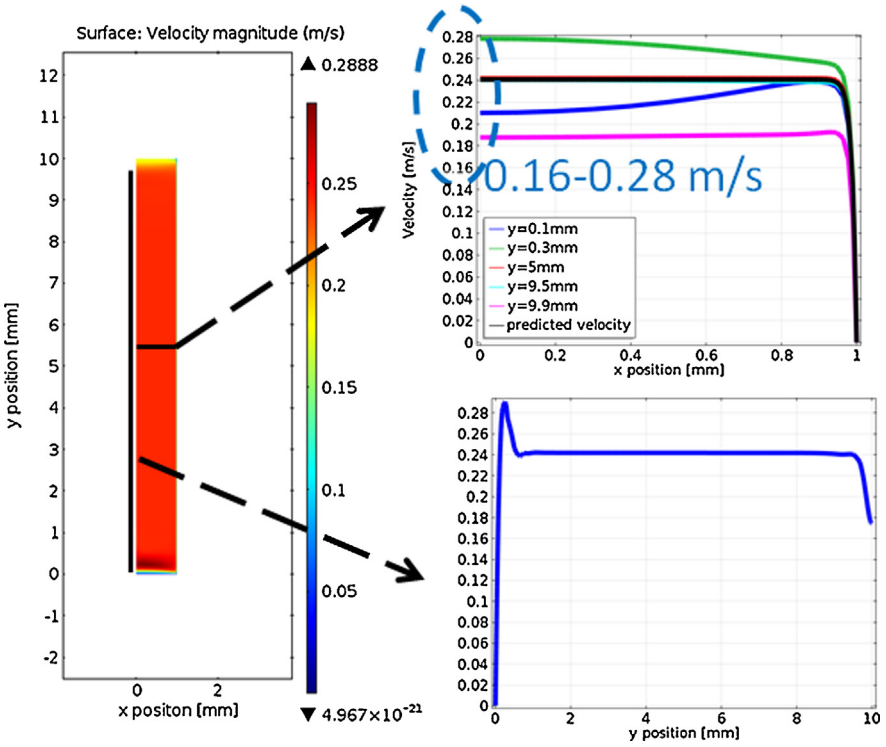

Fig. 2. Verification tests of the thermoelectric MHD flow on an infinite rectangular trench with an open surface. Left: magnitude of the flow velocity on a section of the trench. Top right: velocity profile along x direction at several y positions, and comparison with the theoretical result from [10]. Bottom right: flow velocity along the y direction.

high solubility of LiD compounds [14] at the temperatures relevant for our case. The plasma does not interact chemically with the liquid lithium; only the heat transfer from the plasma to the liquid lithium surface is taken into account. The inclusion of impurities would require distinguishing at least two regimes below and above the solubility limit. Below the solubility limit, and at temperatures below the monotectic temperature (~690 °C), LiD and LiT can be simply treated as soluble chemicals. The solubility of LiD in liquid lithium is a function of temperature, changing from 0.0514 mol.% at 199 °C to 2.08 mol.% at 451 °C [14]. In our device the volume of liquid lithium is 3.41 cm^3 and if we assume a deuterium flux of 1019 $D/cm^2/s$ hitting a 2-cm-wide divertor strike point with a unity deuterium absorption [15], we obtain 19.5 s at 199 °C, and 788 s at 451 °C to reach the solubility limit. In a single plasma discharge of few seconds maximum, the effect of LiD in liquid lithium is negligible. In longer discharges, the impurity effect will have to be taken into account, since it can modify the long term operation of a liquid-lithium PFC device.

3. Results and discussion

A three-dimensional slice of the LiMIT system has been analyzed using the 3D model described in Section 2. The periodicity of the system (see Fig. 1) suggests the most convenient simulation domain, reported in Fig. 3. In Fig. 3, the liquid lithium is represented in blue, the solid metal (stainless steel) in red. The domain includes one trench, half of the metal walls, the four cooling channels, and the surrounding metal structure. The lithium trenches are 5.0 × 2.0 × 80 mm (height × width × length). The total length of the lithium channel, comprising the side channels, is 90 mm. The width of the steel wall is 0.5 mm (only half of the wall is simulated on each side). The top surface of lithium is a slip-wall boundary condition and the side faces of the stainless steel use symmetric boundary conditions. The entire lithium–steel interface uses no-slip boundary condition. The bottom of the whole trench is electrically grounded and other sides are electrically insulated. The top surface receives the divertor heat flux. The other three surfaces are thermally insulated. The divertor heat flux is approximated to a Gaussian heat flux of width 1.0 cm hitting the top surface of the lithium and the steel part,

$$q_{\text{plasma}} = q_0 \exp\left[\frac{(z-0.045)^2}{0.005^2}\right] \text{MW/m}^2 \quad (7)$$

The peak heat flux q_0 is parametrically varied. The heat is exhausted into the four cooling channels, having a local heat transfer coefficient q' which will be varied later for parametric study. In most of this study the local heat transfer coefficient is assumed equal to $q' = 500\,\text{W/(m}^2\,\text{K)}$. This value has been estimated for gas cooling channels. In Section 3.2 we parametrically change this value from 500 to 40,000 W/m^2 K. The coolant temperature is set to be

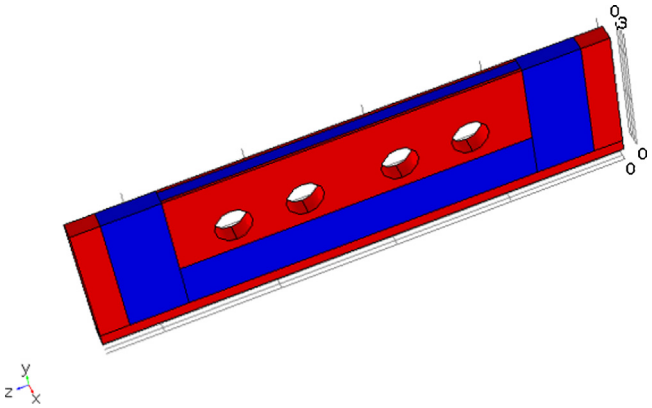

Fig. 3. Simulation domain, comprising the liquid lithium (blue) and the solid metal (red). The domain includes one trench, half of the metal walls, the four cooling channels, and the surrounding metal structure. (For interpretation of the references to color in this figure legend, the reader is referred to the web version of this article.)

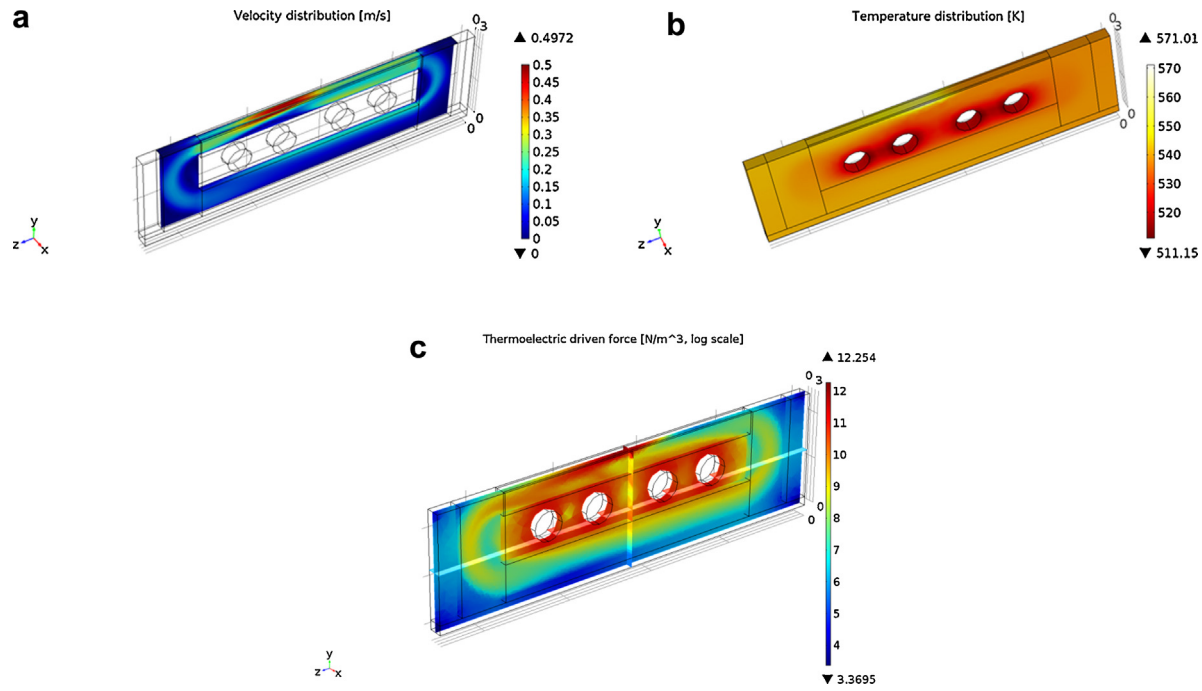

Fig. 4. (a) Flow velocity, (b) temperature, and (c) thermoelectric force (log scale), in LiMIT, as calculated from the 3D model.

293 K, which will also be varied later to study the influence of the cooling efficiency.

Fig. 4 shows an example of calculation, obtained for a peak heat flux of $q_0 = 1.0\,\mathrm{MW/m^2}$, $B = 0.1\,\mathrm{T}$, $q' = 500\,\mathrm{W/(m^2\,K)}$, and trenches of 5 mm height. Fig. 4a shows the magnitude of the fluid velocity. The liquid lithium flows counterclockwise in the figure. The velocity peaks on the downstream of the heated area. This high velocity region is close to the surface and extends into the bulk of the fluid. Fig. 4b shows the temperature field, showing the convective transport due to the lithium flow. Fig. 4c shows the magnitude of the thermoelectric force. The thermoelectric JxB force propels the liquid lithium into the channels. The highest thermoelectric force is close to the Li–SS interface, right under the direct heating region. The region of lithium acceleration extends downstream, as long as the temperature gradient is established at the interface between lithium and stainless steel. Interestingly, a small thermoelectric force is observed also in the return channel at the bottom. Most of the force there is observed at the interface between the two metals. The cooling effect at the interface between the lithium and the wall in proximity of the cooling channels generates a high temperature gradient close to this interface, which in turn produces an acceleration. However, most of the acceleration comes from the direct heating on the top surface and some acceleration exists close to the heat exchange interface between the liquid and the solid parts.

In the following sections, we perform parametric studies to investigate the influence of all the parameters of interest on the performance of LiMIT at steady state. The success of this concept requires a reasonable speed of the lithium flow (at least few mm's per second) even in the fusion-relevant magnetic fields, and a maximum surface temperature of the liquid lithium below <550 °C, or 823 K, to maintain lithium vapor pressure reasonably low. Our parametric study has been done by varying those parameters that most greatly affect the lithium flow and the heat transfer: magnitude of the magnetic field, peak heat flux, trench height, and heat transfer coefficient. The influence of each parameter will be highlighted in the following sections, in order to characterize the trends and identify possible operating ranges. The heat-flux wetter length, although very important, has a similar effect as the peak heat flux: both can change the total power deposition. As a result, this additional parameter can be incorporated in the same trend as the peak heat flux, and it will not be addressed separately. Two scalar variables will be used to present the modeling results: the first is the average lithium velocity in the top trench; the second is the maximum temperature on the lithium surface. The former gives an indication on how fast the top channel can be replenished of lithium. The latter is an important factor to determine the maximum operating range.

3.1. The influence of the magnetic field and the heat flux

The influence of the toroidal magnetic field and the peak heat flux q_0 at the divertor are parametrically investigated in the range $B = 0.0$–$2.0\,\mathrm{T}$, and $q_0 = 1.0$–$10\,\mathrm{MW/m^2}$. In these runs, all the calculations are done for a trench height of 5 mm and heat transfer coefficient $q' = 500\,\mathrm{W/(m^2\,K)}$. These parameters will be sub-optimal, but an optimization of the device is not sought at this stage. Figs. 5–8 report the average lithium velocity in the top trench, and the maximum temperature on the lithium surface, at different magnetic fields and heat fluxes. The results from the 3D simulations (points) are compared to the predictions from a simpler 1D model (solid lines), previously obtained in [7].

Fig. 5 shows the average lithium velocity vs. the magnetic field, for heat fluxes in the range 1.0–$10\,\mathrm{MW/m^2}$. The velocity increases up to a critical field B_{cr}, always below 0.5 T for the heat fluxes of interest. After the critical value, the velocity starts to decrease. In this regime, the increasing MHD drag slows down the motion of the liquid metal. Before the peak, the relation is close to linear, and after the peak the velocity is roughly proportional to a $1/B$ inverse law:

$$B > B_{cr} : \bar{u} \approx \frac{S}{B}\nabla T \tag{8}$$

The 3D simulations and the 1D model give similar peak velocities and similar trends. However, the critical field B_{cr} is different in the two cases. The 1D model predicts that all the peaks occur at the same magnetic field, while the 3D model exhibits a dependence of the B_{cr} on the heat flux. The discrepancies between the two models have not been further investigated, but they can be due either

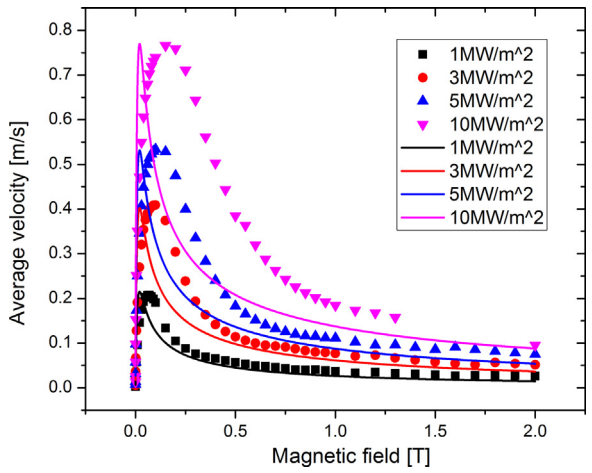

Fig. 5. Average lithium velocity vs. magnetic field, for different peak heat fluxes in the range 1.0–10 MW/m^2. The results from the 3D numerical model (points) are compared to the 1D model (solid lines) obtained in [7]. Simulations are run for heat transfer coefficient q' = 500 W/(m^2 K), and trench height = 5 mm.

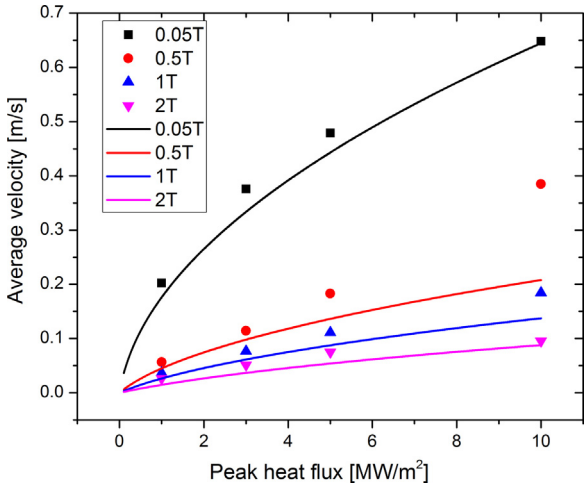

Fig. 7. Comparison of the average lithium velocity vs. peak heat flux, for magnetic fields in the range 0.05 T–2.0 T. The results from the 3D numerical model (points) are compared to the 1D model (solid lines) obtained in [7]. Simulations are run for heat transfer coefficient q' = 500 W/(m^2 K), and trench height = 5 mm.

to the different dimensionality of the two models or to the partial loss in numerical accuracy from turbulence onset at higher flow velocities.

Fig. 6 reports the maximum temperature on the top surface as a function of the magnetic field. The calculation shows that for this sub-optimal configuration the acceptable range T_{max} < 823 K is maintained only at moderate heat fluxes, below <3 MW/m^2. The results from the 3D simulations are compared to the 1D model, showing good qualitative agreement. However, the trends from the 3D runs are richer in features, also exhibiting changes in the derivative.

In Figs. 7 and 8 the average velocity and the maximum top surface temperature are plotted as the function of the peak heat flux q_0. The results from 3D simulations are similar to the 1D model prediction. Both show the same trend and similar peak values. The average lithium velocity increases with the heat flux, but the relation is less than linear, resembling a square-root law. This may lead to a lower fraction of the convection compared to the conduction when the heat flux is high. On the other hand the top surface temperature increases linearly with the incoming heat flux and the value changes little with the magnetic field. At 3 MW/m^2 the maximum temperature is already over 823 K, which is unfeasible for lithium operation in a fusion device. To identify the feasible working regions of LiMIT, the heat transfer coefficient and the trench height are varied to quantify their influence on the design's performance. In the following sections we proceed with a preliminary optimization of the device, characterizing the influence of the heat transfer coefficient of the cooling channel, and of the trench size.

3.2. *Influence of the heat transfer coefficient of the cooling channel*

The heat transfer coefficient of the cooling channel is directly related to the technology used to exhaust the heat (gas cooling, Hypervapotron, T-tubes, etc.). In this section, we assume a fusion relevant condition of B_0 = 1.0 T and peak heat flux q_0 = 10 MW/m^2. The height of the trench is fixed to 5 mm. Three cooling cases are discussed here. First is q' = 500 W/(m^2 K) which corresponds to a normal gas cooling system. The second is q' = 5000 W/(m^2 K) which corresponds to water or other liquid cooling. The third is q' = 40,000 W/(m^2 K) and this value comes from the T-tube cooling

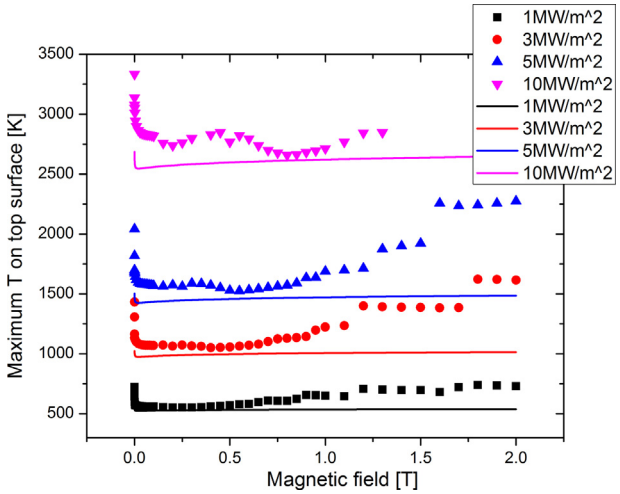

Fig. 6. Maximum top surface temperature vs. magnetic field, for different peak heat fluxes in the range 1.0–10 MW/m^2. The results from the 3D numerical model (points) are compared with the 1D model (solid lines) obtained in [7]. Simulations are run for heat transfer coefficient q' = 500 W/(m^2 K), and trench height = 5 mm.

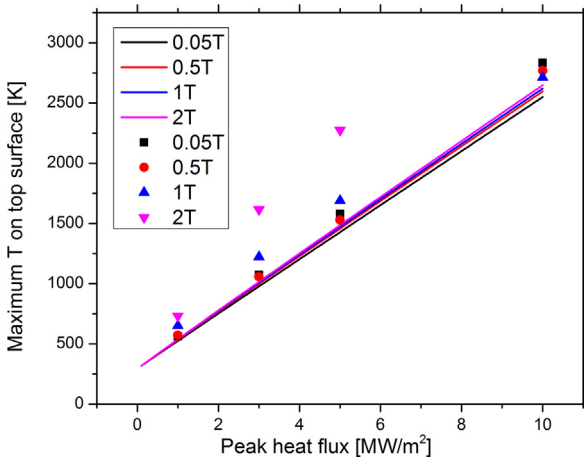

Fig. 8. Comparison of the maximum top surface temperature vs. peak heat flux, for magnetic fields in the range 0.05 T–2.0 T. The results from the 3D numerical model (points) are compared to the 1D model (solid lines) obtained in [7]. Simulations are run for heat transfer coefficient q' = 500 W/(m^2 K), and trench height = 5 mm.

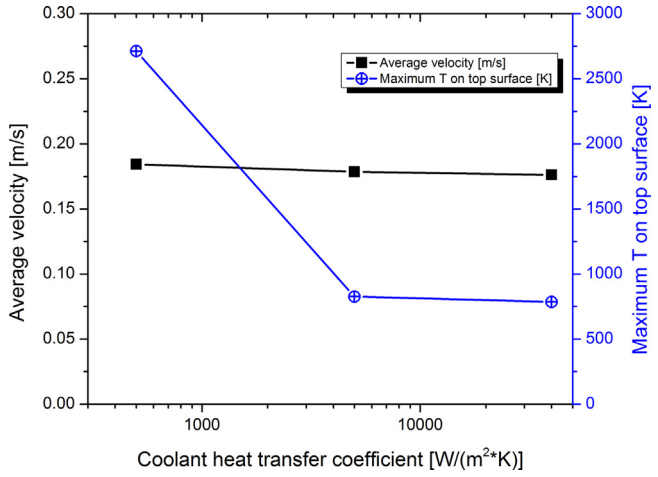

Fig. 9. Influence of the coolant heat transfer coefficient on the average velocity and maximum surface temperature.

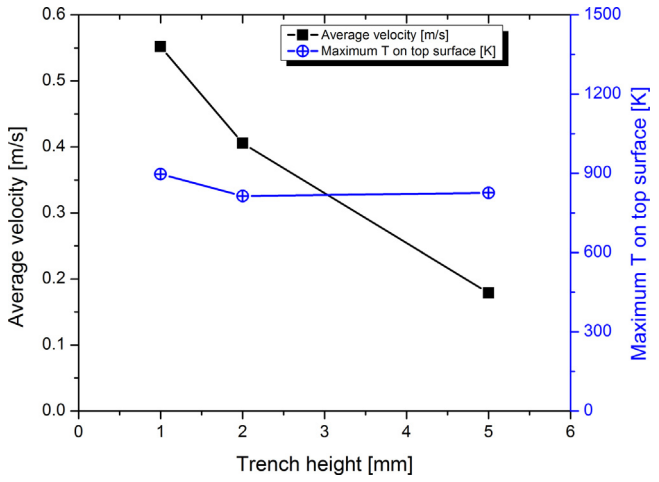

Fig. 10. Influence of the trench height on the average velocity and maximum surface temperature.

concept [16] which has been raised as a cooling method for the divertor target plate. In the first two cases the coolant temperature is 293 K and the coolant temperature of the third case is 453 K which is lithium's melting point to prevent the liquid lithium from solidification.

The influence of the heat transfer coefficient q' is reported in Fig. 9. As expected, the top surface temperature dramatically drops by changing the cooling method. For the last two cases the top surface temperature is around 750 K, within the acceptable range for fusion reactors. The average velocity is only minimally affected, which means that the ability to refresh the lithium is not lowered by increasing the cooling rate.

3.3. Influence of the trench height

Three different trench heights have been investigated, 1 mm, 2 mm, and 5 mm. As in the previous section, we assume a magnetic field of $B_0 = 1.0$ T and peak heat flux $q_0 = 10$ MW/m^2. The heat transfer coefficient is 5000 W/(m^2 K). Fig. 10 reports the results. Varying the trench height has minor effect on the maximum top surface temperature. However, decreasing the trench height greatly increases the lithium flow velocity, which makes the lithium surface refresh faster. Combined with the observations in Section 3.2, it appears that a higher heat transfer coefficient and a lower trench height might be beneficial to the design of an optimal LiMIT system.

3.4. LiMIT performance in 10 s plasma discharge in the HT-7 tokamak

In this final section, we report a simulation in transient conditions for a 10-s plasma shot representative of the HT-7 tokamak. The heat flux and the magnetic field at the HT-7 limiter on the horizontal port have been used. The LiMIT trench is 0.5 mm wide and 1 mm high. The cooling uses 0.4 MPa of compressed air, whose cooling is not enough to take out significant fraction of the heat out of the system in 10 s. The results are reported in Fig. 11. At the final time of the discharge the velocity within the top trench reaches ~0.06 m/s and the velocity in the bottom trench ~0.04 m/s. The maximum temperature is within the acceptable range, with a maximum temperature occurring at the edge.

The flow velocity of liquid lithium driven by TEMHD forces was measured on a LiMIT system installed in the HT-7 tokamak [9]. The tokamak was operated at a toroidal magnetic field of 1.76 T, and it provided a heat flux of 0.5 MW/m^2 [17] on the LiMIT device. The velocity measured from the iCCD camera during the HT-7 experiment is 0.037 + −0.005 m/s. From our model we calculate a velocity of ~0.06 m/s on top of the lithium channel after 10-s of plasma shot at constant heat flux. The calculated value is higher than the experimental value of a factor of 2×. A possible reason for this discrepancy is that the HT-7 discharge last around 0.9 s; the time at which the measurement was taken is unknown, and can be any value between zero and 0.9 s. We argue that the measurements were taken at an

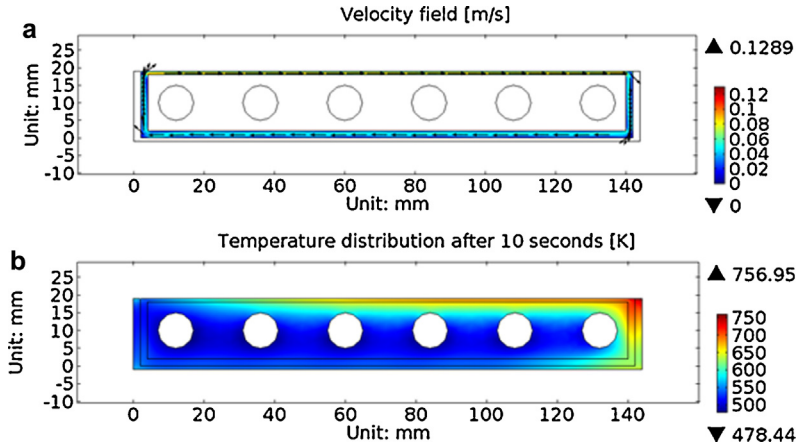

Fig. 11. (a) Velocity and (b) temperature of the cross section of the trenches after 10 s HT-7 plasma shot.

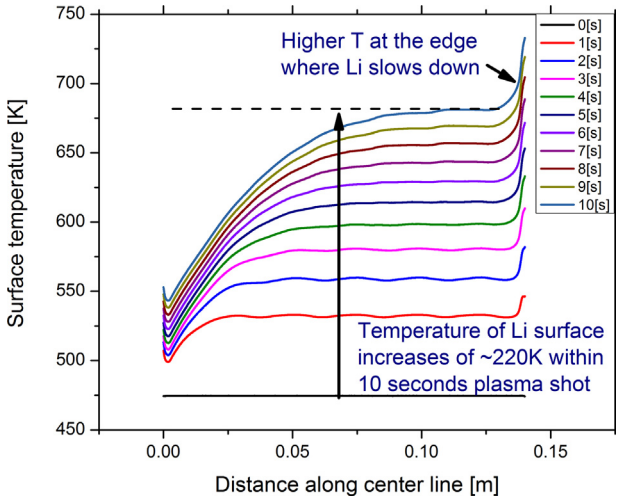

Fig. 12. Temperature increase of lithium during a 10-s plasma shot in HT-7, along a longitudinal line on the top surface at the center of trench.

early stage of the discharge, when the lithium was still accelerating. The result from the transient simulation shows that it takes about 1 s to reach the ~0.06 m/s velocity. At the time of the measurement the lithium was still accelerating and it did not reach the calculated steady-state velocity.

Fig. 12 shows the temperature of the lithium surface along a longitudinal line on the top surface at the center of the trench. The curves are plotted one per each second. The lithium temperature increases of ~220 K after 10 s of discharge. The highest temperature happens at the edge, where lithium slows down before entering the return flow trenches. The velocity and maximum temperature are acceptable for HT-7 and current fusion reactors working in transient conditions.

An interesting effect observed in the transient simulations, is the asymmetry of the temperature profile. The profile is flat on the downstream side, while it is much steeper on the upstream side. This asymmetry may cause strong thermoelectric current flowing toward the upstream side and in turn generate a thermoelectric force pointing into the trench. Whether this force can stabilize the surface or squeeze the lithium flow needs further investigations.

4. Conclusions

Simulations of the physics of the LiMIT device (Lithum-Metal Infused Trenches) have been done using COMSOL, by solving the three-dimensional physics of the thermoelectric-driven MHD liquid-lithium flow in open metal trenches. At first, the 3D model has been verified against the analytical solution found by Shercliff. Then, parametric studies versus the heat flux and the magnetic field have revealed the trends of the average lithium velocity and of the maximum lithium temperature reached during plasma exposure. The velocity increases up to a critical field B_{cr}, always below 0.5 T for the heat fluxes of interest. After the critical value, the velocity decreases, mainly due to MHD drag. In sub-optimal design, the lithium temperature easily exceed the acceptable operational range of $T_{max} < 550\,^{\circ}C$. However, further parametric studies versus the heat transfer coefficient of the cooling channel reveal that the surface temperature of lithium dramatically drops by changing the cooling method. High heat transfer coefficients of the cooling channel ($q' > 4000\,W/m^2\,K$) and smaller trench heights lead to acceptable performance with heat fluxes up to 10 MW/m^2. The constraints are much milder in transient conditions; the simulation of a transient case has been reported for a 10-s plasma shot, representative of the LiMIT operations during an HT-7 discharge, finding acceptable velocities and temperatures for the HT-7 machine and current fusion reactors working in transient conditions.

Acknowledgements

The author would like to thank the visualization lab of Beckman Institute of University of Illinois at Urbana-Champaign for providing the usage of COMSOL. This work is supported under DOE contracts DE-FG02-99ER54515.

References

[1] M. Greenwald, R. Callis, D. Gates, B. Dorland, J. Harris, R. Linford, et al., Tech. Rep. Fusion Energy Sci. Advisory Committee (2006).
[2] M.A. Abdou, The APEX TEAM, A. Ying, N. Morley, K. Gule, S. Smolentsev, et al., Fusion Eng. Des. 54 (2001) 181.
[3] D.K. Mansfield, D.W. Johnson, B. Grek, H.W. Kugel, M.G. Bell, R.E. Bell, et al., Nucl. Fusion 41 (2001) 1823.
[4] M.L. Apicella, G. Apruzzese, G. Mazzitelli, V. Pericoli Ridolfini, A.G. Alekseyev, V.B. Lazarev, et al., Plasma Phys. Control Fusion 54 (2012) 035001.
[5] M. Nieto, D.N. Ruzic, W. Olczak, R. Stubbers, J. Nucl. Mater. 350 (2006) 101–112.
[6] D.N. Ruzic, M. Nieto, J.P. Allain, M.D. Coventry, J. Nucl. Mater. 313-316 (2003) 646–650.
[7] D.N. Ruzic, W. Xu, D. Andruczyk, M.A. Jaworski, Nucl. Fusion 51 (2011) 102002.
[8] W. Xu, D. Curreli, D. Andruczyk, T. Mui, R. Switts, D.N. Ruzic, J. Nucl. Mater. 438 (2013) S422–S425.
[9] J. Ren, J.S. Hu, G.Z. Zuo, Z. Sun, J.G. Li, D.N. Ruzic, et al., First results of flowing liquid lithium limiter in HT-7, Phys. Scr. T159 (2014) 014033.
[10] J.A. Shercliff, J. Fluid Mech. 91 (1979) 231.
[11] M.A. Jaworski, T.K. Gray, M. Antonelli, J.J. Kim, C.Y. Lau, M.B. Lee, et al., Phys. Rev. Lett. 104 (2010) 094503.
[12] R. Kaita, R. Majeski, T. Gray, H. Kugel, D. Mansfield, J. Spaleta, et al., Phys. Plasma 14 (2007) 056111.
[13] W. Xu, V. Surla, M.A. Jaworski, M. Lee, T. Mui, M.J. Neumann, et al., J. Nucl. Mater. 415 (2011) 981.
[14] E. Veleckis, R.M. Yonco, V.A. Maroni, J. Less-Common Metals 55 (1977) 85–92.
[15] C. Liao, M.S. Kazimi, J.E. Meyer, Fusion Sci. Technol. 23 (1993) 208.
[16] S.I. Abdel-Khalik, Thermal-hydraulic studies in support of the aries CS T-tube divertor design, Fusion Sci. Technol. 54 (2008) 864–877.
[17] Q. Li, H. Chen, P. Qi, Z.H. Yang, G.N. Luo, H.Y. Guo, Fusion Eng. Des. 85 (2010) 126–129.